Prospect Planck Morphology

Morphology of the CMB in a Universe with non–trivial topology

Martin France

Supervised by: **Thomas Buchert**

UCBL Lyon 1, Centre de Recherche Astrophysique de Lyon

Working Group in Morphology,
manuscript in progress, July 2010

Contents

1 Introduction

With the observational CMB data harvested between 1990 and 2010, by COBE, WMAP, many ground based instruments, and now Planck, Cosmology enters a new era said as era of Precision Cosmology. These Cosmic Microwave Background data afford tighter constraints to the models of Cosmology. Cosmology becomes an observational science for the largest scales, although, it is not an experimental science since only one realization is made available of this oldest physical process one would observe. The CMB curve (spectral volumic energy density) matches to the Planck distribution of an apparent black body having a temperature of $T_{obs} = 2.725\ K\ +/-0.0001$. Apparent, as one measures today only the elongated wavelengths of a real black body at $T_{emi} \approx 3000\ K$, at a redshift ($z \approx 1100$) when matter and radiation are in thermal equilibrium. When the temperature falls to this value of T_{emi} , the radiation pressure, that disabled the electron to bind to the nucleus before, is now just sufficiently too weak and the atoms form sustainedly, leaving the photons propagating freely in the Universe [1]. These photons reach us after a more or less eventful travel, forming this CMB wavefront that one analyses through the CMB maps.

This CMB wavefront, object of many studies, shows difficulties to fit to the Standard model of Cosmology and to the Standard model of Particle Physics. However, new models built from Cosmic Topology develop simulations conforming better to the observations than the Concordance model with trivial topology. Putting into prospect the arrival of the soon to come Planck data, we introduce here the beginning of a systematic study *Prospect Planck Morphology* with the aim to develop a robust morphological characterization of the CMB wavefront based upon enhanced Minkowski functionals. The study of new morphological signatures will be a target for this project.

[1]Another primeval physical transition would offer another single realization in the Universe: this is the equivalence matter–radiation transition almost contemporary to the matter–radiation decoupling of the CMB. Depending on the ratio of the number of photons by nuclear particle, the moment of this transition would occur slightly before ($z \approx 1300$) the CMB at a temperature of 4000 K (for 10^9 photons by nuclear particle). Or would take place after the transparency threshold of the CMB for a ratio of 10^{10} photons by nuclear particle when the Universe cooled down to 400 K.

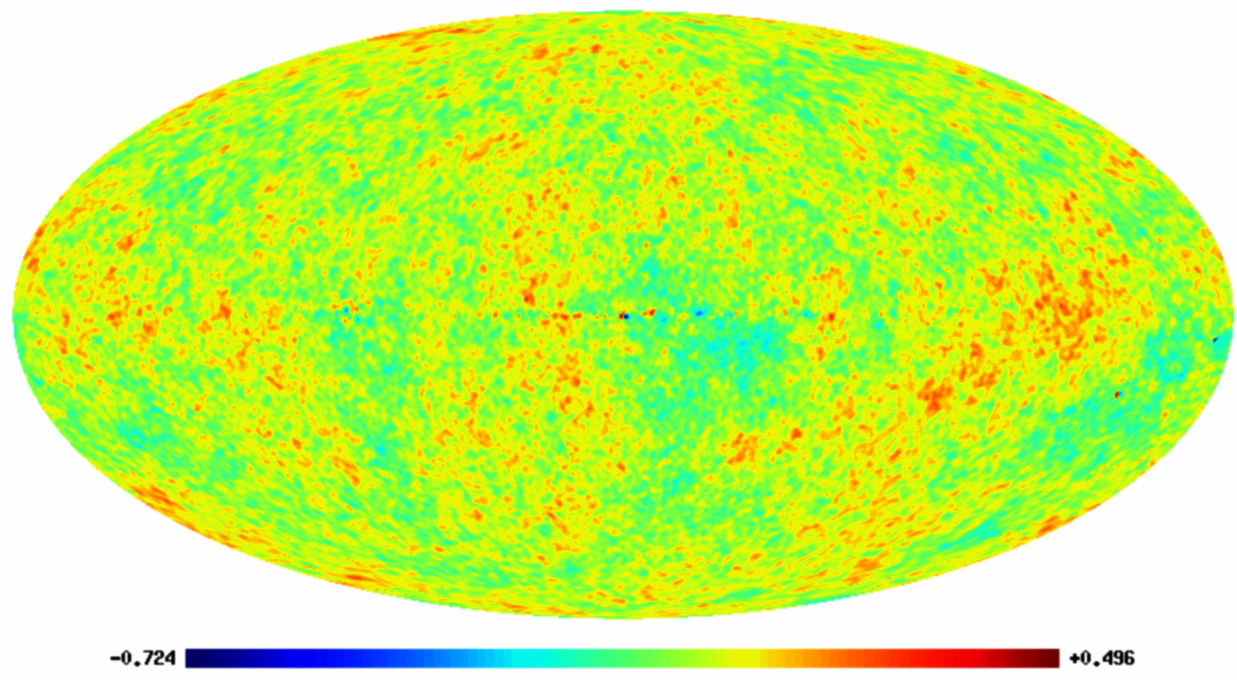

Figure 1: WMAP ILC 7 year parametrized to $l_{max} = 900$

However, let us first have, in the present document, a tighter view over the available data, the analysis tools and a first application using the Torus model. We adopt here a triple point of view on the CMB through the *2–point auto–correlation functions*, *angular power spectra* and *Minkowski functionals* for:

α – The Wilkinson MAP data analysis (for the 3,5 and 7 years data release)

β – The ΛCDM model data analysis

γ – The Torus model data analysis (with one choice of periodicity length)

Concerning the morphological analysis and the Minkowski functionals, the reader may usefully refer to the Memorandum written with Thomas Buchert in late march 2010 [FRA-1].

2 CMB observations and model simulations; Data and Codes

2.1 The observation space and the dipole issue

CMB displays as a wavefront upon the celestial shell surrounding the observer. The observer has a proper movement relative to the surrounding CMB and one probably cannot have a complete knowledge of the components of this movement. Therefore, in the detail, due to this displacement of the Earth relative to the cosmic background, the shape of this celestial shell would be considered as a complex closed surface in general. The commonly accepted assumption considers this shell as a sphere. Though, many problems arise to hold that premise. In the 2-point autocorrelation function, the dipole is the content in correlation for the angular scale π. One build the overall dipole from contributions that are more or less reachable or knowable. The CMB dipole will be estimated from a jigsaw puzzle made of WMAP spacecraft proper motions and instrumental biases denoted as pseudo-dipoles. The CMB dipole signal is at first order contaminated by Doppler-Fizeau effect due to the motion of WMAP in the galaxy. For a dual antenna instrument such as WMAP, having the two unit direction vectors n_A and n_B, one write the dipole difference signal d as:

$$d = \frac{\tilde{T}}{c}\; v\; (n_B - n_A)$$

Where $\tilde{T} = 2.725K$ is the CMB monopole, v is the joint velocity and c is the speed of light.

This only bias shows a magnitude ten to twenty times bigger than the expected CMB anisotropies [LIU-1]. To mention also, a seven arc-minutes error upon the WMAP line of sight deviates the CMB dipole in a range of ten to twenty μK, to compare to twenty μK which is the WMAP probe temperature sensitivity (two μK for Planck).

But, this overall dipole component ($l = 1$) being substracted from the CMB autocorrelation function, most of the observational studies made upon the CMB assume that we sit at the center of a sphere. Relying upon this, physics, softwares, data for the CMB study are developed and made available using the HEALPix package which projects the CMB sphere upon a pixel grid. The HEALPix projection proceeds at constant pixel surface area and isolatitude repartition [GOR-1]. The admitted sphere and this common tool offer a powerful referential for the comparative investigations of the CMB.

2.2 Building the angular power spectrum and the $2{-}pcf$

The 2–point auto–correlation function (thereafter $2-pcf$) and the multipole power spectrum are tools naturally or natively developed for the work upon the unitary sphere. For each available angular scale ϑ in the discretized CMB map, the $2-pcf$ calculates straightforwardly as:

$$C(\vartheta) = <\Delta T(\vec{n}(\theta_1,\phi_1))\ \Delta T(\vec{n}(\theta_2,\phi_2))>$$
$$\text{with} \quad \vec{n}(\theta_1,\phi_1)\ .\ \vec{n}(\theta_2,\phi_2) = cos(\vartheta)$$

Where the unitary vector $\vec{n}(\theta,\phi)$ is the direction of the observed photon and $\Delta T = T - \tilde{T}$ is the temperature anisotropy.

A strong assumption based upon our present CMB observations data and theoretical fundaments drives us to consider the CMB random field as described with f, a class of functions verifying the Laplace equation:

$$\Delta(f(\theta,\phi)) = 0, \quad \forall(\theta,\phi)$$

These regular functions f fit well to the CMB overall properties of statistical homogeneity and statistical isotropy, and can take into account some slight anisotropies and irregularities over the random field. Such a functions are said harmonic, and have the following decomposition in spheric harmonics series [2]:

$$f(\vec{n}(\theta,\phi)) = \sum_{l=0}^{\infty}\sum_{m=-l}^{m=+l} a_{l,m} Y_{l,m}(\theta,\phi)$$

The coefficients $a_{l,m}$ are independent random variates and the complex $Y_{l,m}$ are the solid harmonics of degree l and order m:

[2] The spherical harmonics form a complete set of orthonormal functions and provide an orthonormal basis of the Hilbert space of square-integrable functions.

$$Y_{l,m} = Ne^{im\phi}P_{l,m}(cos(\theta))$$

N is a normalization constant, and $P_{l,m}(cos(\theta))$ an associated eigenfunction.

One may expand now the function of temperature anisotropy $\Delta T(\theta, \phi)$ over the CMB sphere:

$$\Delta T(\theta, \phi) = \sum_{l=0}^{\infty}\sum_{m=-l}^{m=+l} a_{l,m}Ne^{im\phi}P_{l,m}(cos(\theta))$$

While one write the eigenfunctions $P_{l,m}(x)$ from the Legendre polynomials $P_l(x)$ which are eigenfunctions of the Legendre ODE.

Finally we have:

– The angular power spectrum which is:

$$C_l = \frac{1}{2l+1}\sum_{m=-l}^{m=+l} \mid a_{l,m} \mid^2$$

– The 2-point auto-correlation function expands as:

$$C(\vartheta) = \sum_{l=0}^{\infty} C_l \frac{2l+1}{4\pi} P_l(cos(\vartheta))$$

2.3 Quantification of the anisotropies

Measurements of anisotropies and inhomogeneities in various-scale distribution of matter in the Universe are certainly not compatible with the uniformous primeval Cosmic Microwave Background.

However, the CMB uniformity is frequently quantified in term of Gaussianity, and its slight anisotropies are therefore evaluated in term of non-Gaussianity [3] which is compatible with the mathematical formalism for the

[3] However, as mentionned by Komatsu, one must distinguish between non-Gaussianity and a violation of statistical isotropy [KOM-1].

description of the CMB temperature fluctuations ΔT relying upon the paradigm of a zeroed Laplacian described above.

The prior of harmonic functions, does not leave no place for temperature irregularities or even singularities within the CMB wavefront mathematical description, as such observables would not verify a property of the harmonic function which is; *the average value taken around a point equals the value taken at that point.* One talk of temperature fluctuations only. Moreover, the availability of one realization of the CMB only, limits the validity of a study of Gaussianity to the sub-sampled processes. Nevertheless, let us first having a rapid description of the CMB anisotropies and inhomogeneities in the frame of Gaussian distribution study. The concept of CMB Gaussianity can be approached using different random variables:

1 – Census of temperature without spatial correlation analysis

Gaussianity expresses as:

$$P(T) = \frac{1}{\prod_{i,j\ \ i\neq j}^{n} [\sigma_{i,j}\ \ (2\pi)^{\frac{n(n-1)}{4}}]} exp^{[-\frac{1}{2}\sum_{i,j\ \ i\neq j}^{n} \frac{|\Delta T_{i,j}|^2}{\sigma_{ij}^2}]}$$

Where n is the number of distinct temperature values present in the probed samples of the CMB. The shift to this one-point distribution function relative to the CMB data reveals only a global behaviour in the space of temperatures. No local singularity such as the cold-spot area [SOL-1] can be detected with this tool.

2 – CMB temperature distribution with spatial correlation analysis

The 2-point auto-correlation function adds to the previous tool the knowledge in angular scale content. With the angular power spectrum related to this $2-pcf$, the 1° ($l \approx 180$) angular scale dominates in the CMB, although, the phase information being absent, no evidence is made of CMB local singularities (at 1°) neither.

For the $2-pcf$, Komatsu [KOM-1] constrains the Gaussianity of the CMB temperature *anisotropy* $\Delta T(\vec{n}(\theta,\phi))$ to the following probability density function:

$$P(\Delta T) = \frac{1}{|\xi|^{1/2}\ (2\pi)^{\frac{N_{pix}}{2}}} exp^{[-\frac{1}{2}\sum_{i,j\ i\neq j}^{n} \Delta T_i\ (\xi^{-1})_{i,j}\ \Delta T_j]}$$

Where $\xi_{i,j} =< \Delta T_i \Delta T_j >$ is the covariance matrix (the $2-pcf$) of the temperature anisotropy and $\mid \xi \mid$ the determinant of ξ.

Given that the same points distributed different ways show the identical $2-pcfs$, the content in structures of a random field, can not be described by the $2-pcf$, neither its angular power spectrum, nor the related Gaussian probability density function of ΔT.

The 3-point auto-correlation function (bispectrum) permit a first description of the content in structures of the CMB random field.

Graphical representation

2.4 The scalar valued Minkowski functionals

The morphological analysis using the Minkowski functionals tool has to take into consideration the projection of the pixel grid upon a space of non zero constant curvature (the admitted sphere) [SCH-1][FRA-1], as it was worked out primarily upon a flat N–dimensional space.

3 The Torus model

The fundamental domain of a Torus model is a cube determined by the size of its side L (in units of the Hubble length c_0/H_0). In such a multi–connected Universe, our CMB sphere (which has a diameter D) may interpenetrate, as a function of the ratio L/D, different numbers of neighboring spheres or none. As each sphere is an isolated system, this drives to the conclusion that the intersections areas between spheres are a peculiar domain showing specific properties. Not making a development here, we mention only that: First, these junctions are materialized by ellipses or circles (intersection of two spherical or ellipsoidal shells). Secondly, light can not propagate through the shell but it can travel along the boundary (the ellipse or intricated ellipses). Third, the finite size of the fundamental domain fixes the biggest wavelength of any signal to L and settles eigen–modes [AUR-1][AUR-2][AUR-3].

Thus, observational consequences of the Torus model upon the CMB wavefront are huge as one expects therefore:

– an oscillatory behavior of the angular power spectrum due to the discrete k–spectrum

– suppression of the CMB power at large angular scales (low multipole)

– observable pattern of intersecting (ellipses) circles

The Torus comparison with WMAP observations and the ΛCDM infinite Universe goes toward the detection of these expectations through the 2–point auto–correlation function (2–p.a.c.f.) displayed in *Figure* 2. This figure shows the small ripples of the Torus 2–p.a.c.f. absent in the WMAP and ΛCDM curves. Moreover, the overall extinction of the angular power of the Torus is strong. Other realizations of the Torus model are currently probed and other sizes of the fundamental domain L are endeavored.

The Torus (1 Hubble length) angular power spectrum (*Figure* 3) displays the emphasized small angular scales, moreover, the large scales vanish faster than for the ΛCDM model.

3.1 Data and Codes

α - The Wilkinson MAP:

The five bands of the WMAP instrument (see the CMB probes table in Section 5) provide each a sky temperature map (denoted I map) where the CMB dipole has been removed [4]. Each Internal Linear Combination map (denoted ILC map) results of the weighted linear combination from the five smoothed (1° then 1.5° kernel) maps [WMA-1] and substract the foreground.

[4] Angular resolution θ and maximum multipole value are linked by the law: $l_{max} = \frac{180}{\theta}$ () .

These ILC maps are only used for overall studies of the random Gaussian field as the resolution is limited. For the accurate study at $0.2°$ resolution, one uses the 'Combined TT power spectrum' data which provide the multipole (therefore angular) power spectrum (beginning for $l = 2$ as the dipole is removed) and the 'crude' estimate of the errors. The cosmic variance is therefore only taken into account by these error data.

The WMAP general science data repositories:

– 3 year v2: http://lambda.gsfc.nasa.gov/product/map/dr2/

– 5 year v3: http://lambda.gsfc.nasa.gov/product/map/dr3/

– 7 year v4: http://lambda.gsfc.nasa.gov/product/map/dr4/

β – The ΛCDM model data:

The Cosmological parameters set are exhaustively entered within the following web interface to produce the corresponding CMB data of a sharpened ΛCDM model:

– ΛCDM model data and online toolbox:
http://lambda.gsfc.nasa.gov/toolbox/

We used a relevant set of Cosmological Parameters as described in the three following papers [LAR-1][JAR-1][KOM-2].

γ – The Torus model data and codes:

Data and specific codes where made available by Sven Lustig at Ulm University: Sven Lustig <sven.lustig@uni-ulm.de>

4 Preliminary Results

4.1 The Torus compared to ΛCDM and WMAP

4.1.1 2–point auto–correlation function

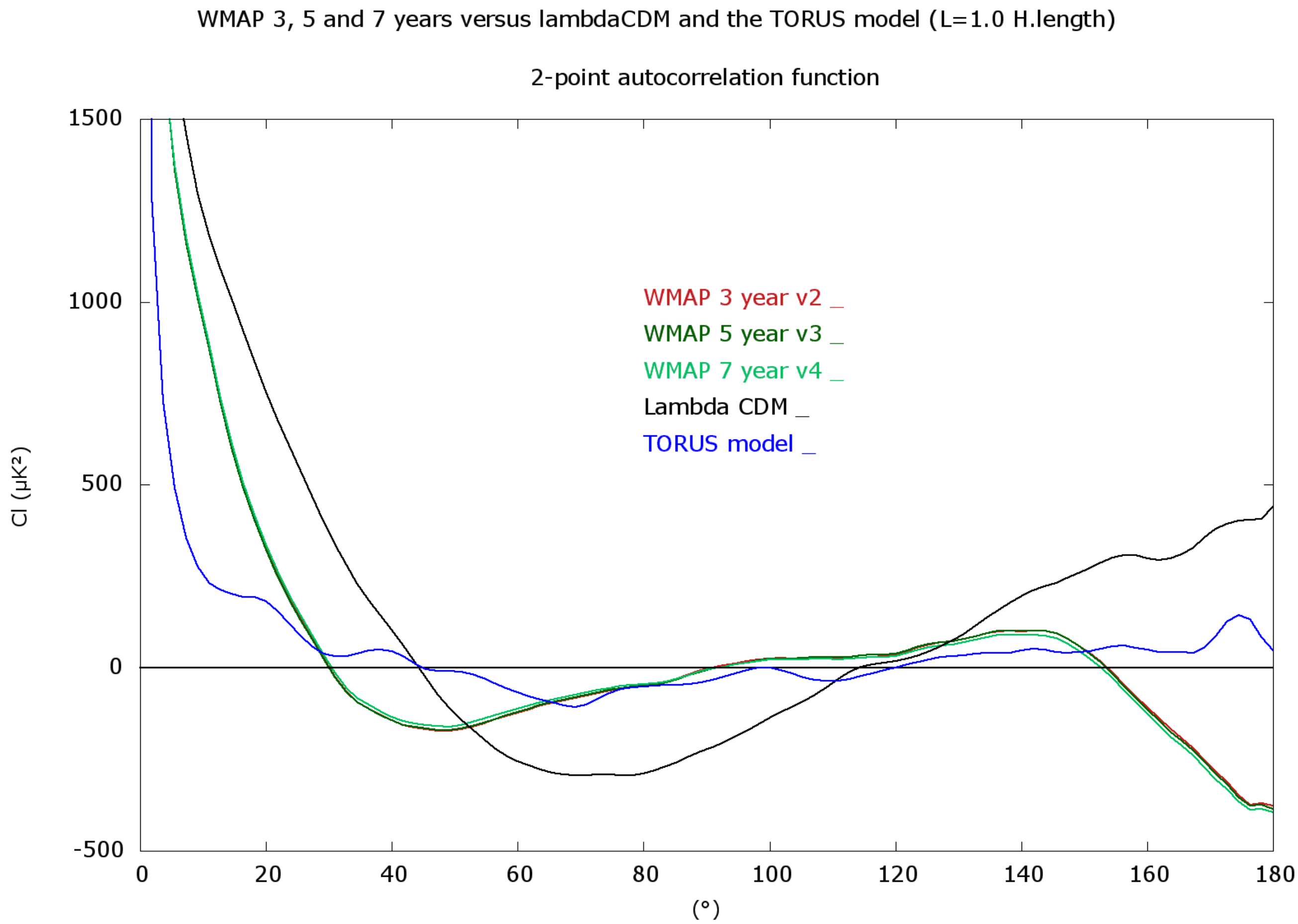

Figure 2: All the maps are analyzed with the same value of l_{max} at 900. The Torus model is calculated using $10,000$ eigenvalues, it lies closer to the WMAP observation data than the ΛCDM model. Standard ΛCDM model parameters (WMAP+BAO+H_0) are referenced in [LAR-1][JAR-1][KOM-2]. Torus model *alm* dataset: Sven Lustig. Correlation function code: Sven Lustig.

4.1.2 Angular power spectrum

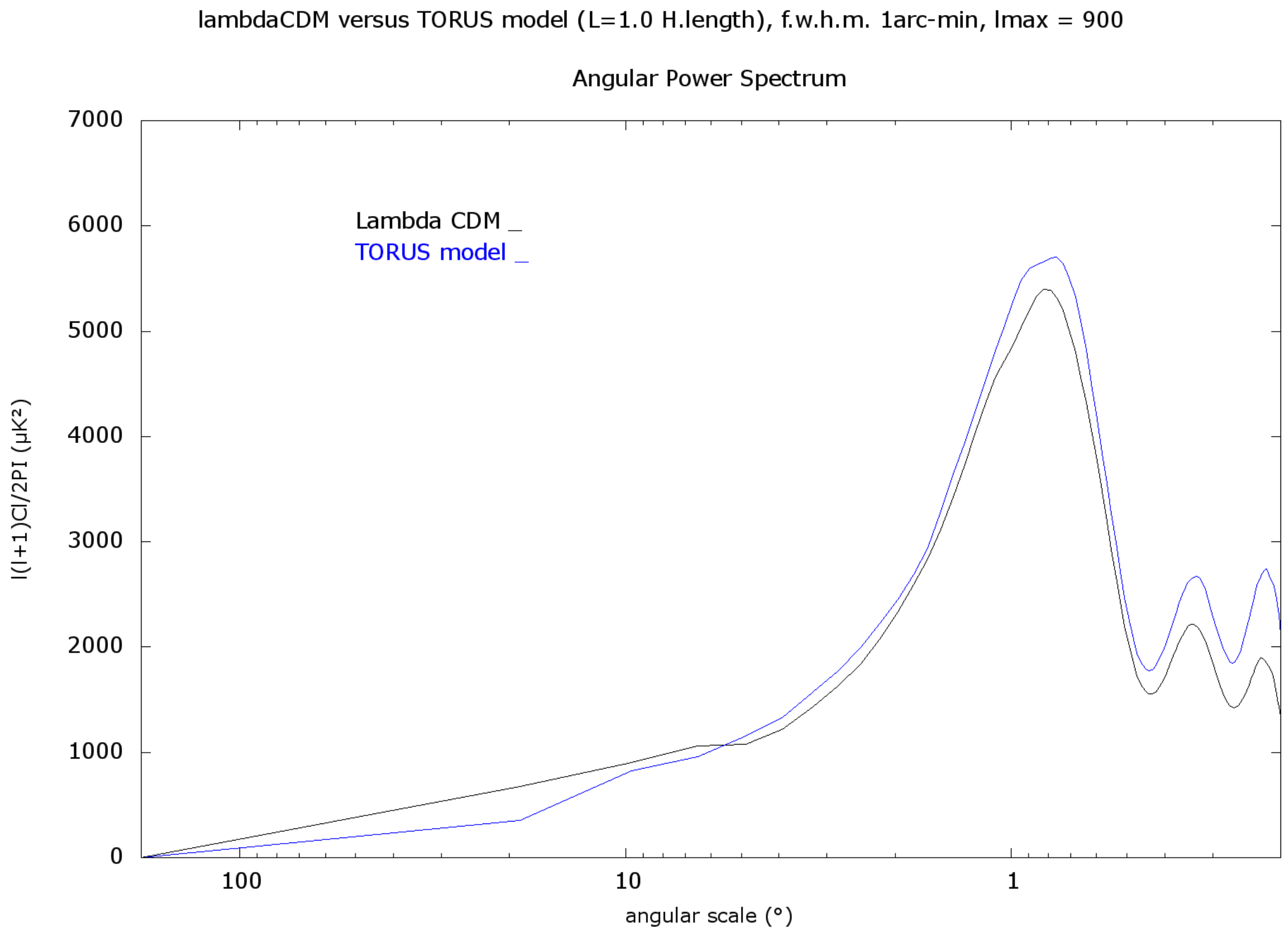

Figure 3: All the maps are analyzed with the same ceiling value of l_{max} at 900, not taking into account the extended multipole data (from ground based or balloon born instruments) there. The Torus model is calculated using also 10, 000 eigenvalues. Torus model *alm* dataset: Sven Lustig. Power spectrum code: Sven Lustig.

4.2 Minkowski functionals analysis

4.2.1 WMAP 3, 5 and 7 years

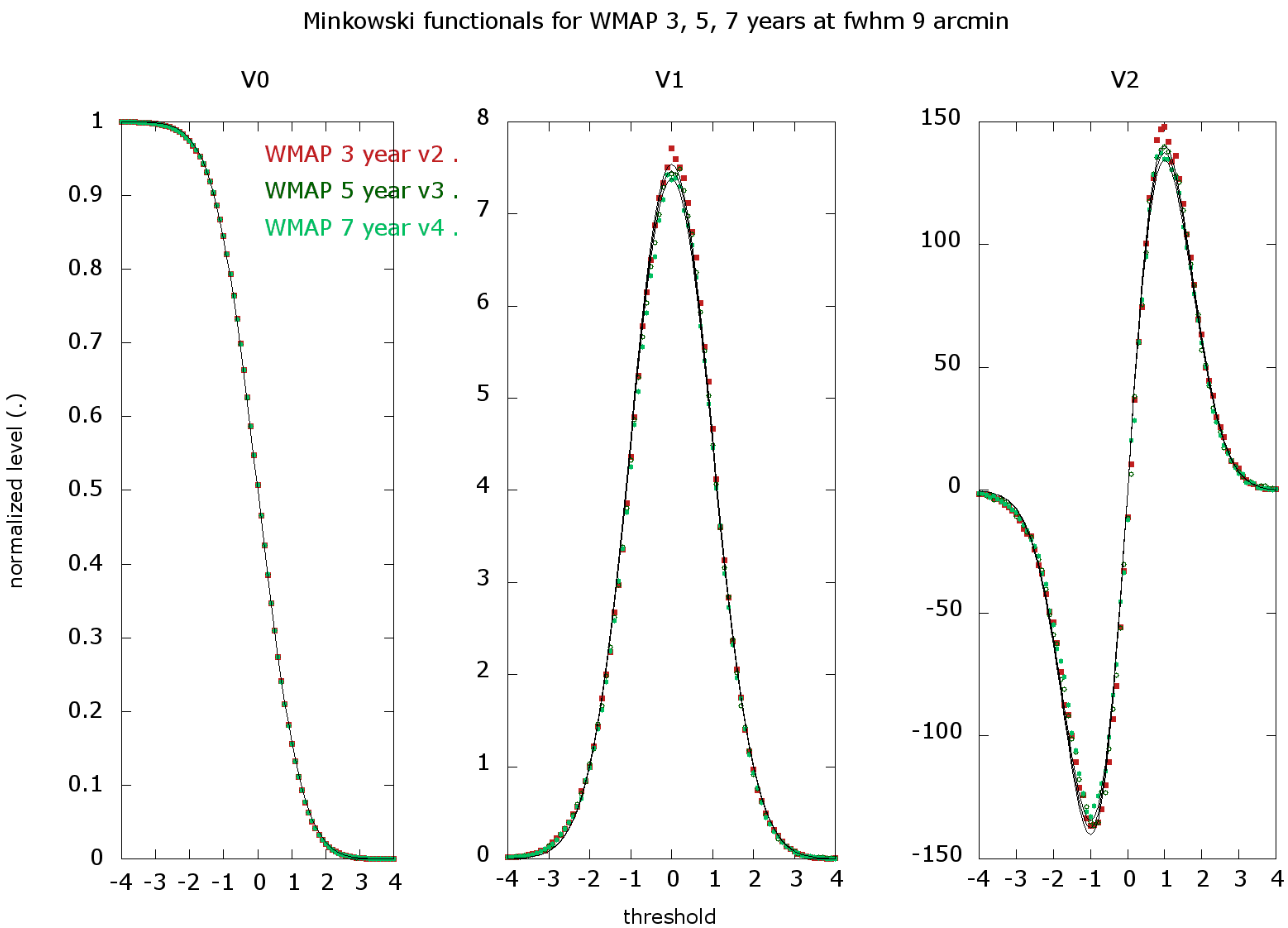

Figure 4: The Minkowski functional analysis confirms the similarity of the WMAP ILC data for the 3, 5 and 7 year sets. Minkowski functional code: Holger Janzer.

4.2.2 The Torus compared to ΛCDM

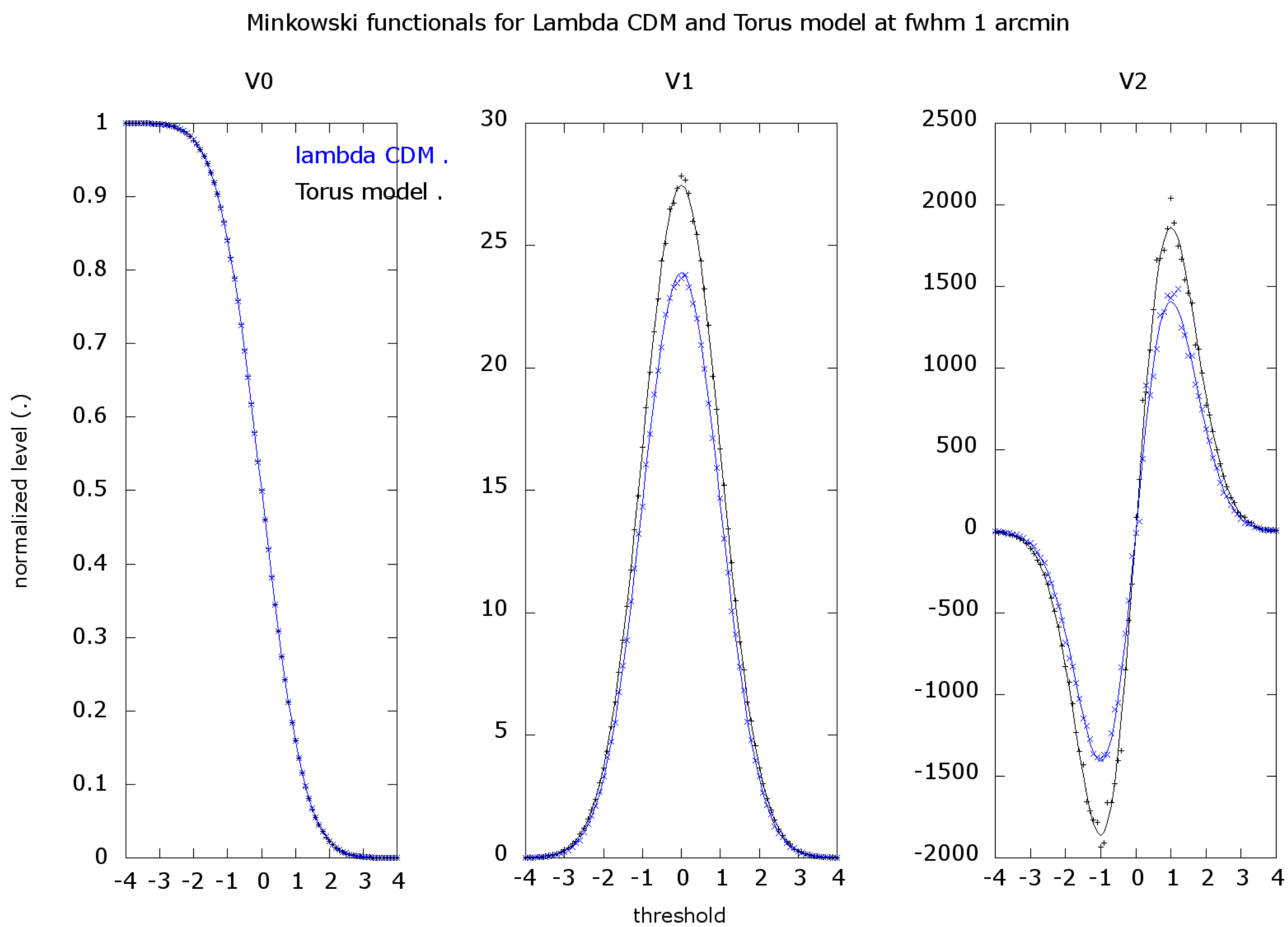

Figure 5: The Minkowski functional analysis shows the different behaviors of the Torus and the ΛCDM, but both seem to stay rather Gaussian. Minkowski functional code: Holger Janzer.

References

[AUR-1] R. Aurich, S. Lustig, F. Steiner, and H. Then, *CMB Alignment in Multi-Connected Universes*, arXiv:astro–ph/0612308v1 12 Dec 2006.

[AUR-2] R. Aurich, H. Janzer, S. Lustig, and F. Steiner, *Do we live in a small Universe*?, arXiv:0708.1420v2 [astro–ph] 8 Apr 2008.

[AUR-3] R. Aurich, *A spatial correlation analysis for a toroidal Universe*, arXiv:0803.2130v2 [astro–ph] 30 Jul 2008.

[LAR-1] D. Larson, *Seven–Year WILKINSON MICROWAVE ANISOTROPY PROBE (WMAP1) observations: power spectra and WMAP–derived parameters*, arXiv:1001.4635v1 [astro–ph.CO] 26 Jan 2010.

[JAR-1] N. Jarosik, *Seven–Year WILKINSON MICROWAVE ANISOTROPY PROBE (WMAP1) observations: Sky Maps, Systematic Errors, and Basic Results* , arXiv:1001.4744v1 [astro–ph.CO] 26 Jan 2010.

[KOM-1] E. Komatsu, *Hunting for primordial non-Gaussianity in the cosmic microwave background*, arXiv:1003.6097v1 [astro–ph.CO] 31 Mar 2010.

[FRA-1] M. France, T. Buchert *Memorandum: Morphological characterization using the Minkowski Functionals*, CRAL Mar 2010.

[GOR-1] K.M. Gorski et al., *HEALPix: A framework for high–resolution discretization and fast analysis of data distributed on the sphere*, arXiv:astro–ph/0409513v1, 21 Sep 2004.

[SCH-1] J. Schmalzing, K.M. Gorski, *Minkowski Functionals used in the morphological analysis of Cosmic Microwave Background Anisotropy Maps*, arXiv:astro-ph/9710185v2, 20 Dec 1997.

[WMA-1] The *WMAP* Science Working Group, *WILKINSON MICROWAVE ANISOTROPY PROBE (WMAP) Explanatory Supplement*, 11 Feb 2003.

[LIU-1] H. Liu, T. Li, *Pseudo-Dipole Signal Removal from WMAP Data*, arXiv:1005.2352v2 [astro–ph.CO] 17 May 2010.

[KOM-2] E. Komatsu, *Seven–Year WILKINSON MICROWAVE ANISOTROPY PROBE (WMAP1) observations: cosmological interpretation*, arXiv:1001.4538v2 [astro–ph.CO] 12 Feb 2010.

[SOL-1] D.I. Solov'ev, O.V. Verkhodanov, *Statistics of Extragalactic Objects in the Cold Spot Region on the CMB Maps*, ISSN 1990-3413, Astrophysical Bulletin, 2010, Vol. 65, No. 2, pp. 121âĂŞ131. c Pleiades Publishing, Ltd., 2010.

5 CMB probes

probe (instr.)	years	final res. FWHM (°)	l multi-pole ()	temp. sens. (μK)	wavelength band																	
					nb	central frequency (GHz)																
						22	30	31	40	44	52	60	70	81	90	100	143	217	353	545	857	
						angular resolution (°)																
COBE (DMR)	1989-1993	7	26	300	3			7.0			7.0			7.0								
WMAP	2001-	0.2	900	20	5	0.93	0.68		0.53			0.35			0.23							
Planck (LFI) (HFI)	2009-	0.08	2250	2	9		0.55			0.4			0.23			0.17	0.11	0.09	0.08	0.08	0.08	